MODELLING THE VERTICAL DYNAMICS OF PHYTOPLANKTON POPULATIONS IN FRESHWATER SYSTEMS

Alison Peard

Student No: 115379106

SCHOOL OF MATHEMATICAL SCIENCES

UNIVERSITY COLLEGE CORK

January 2020

Acknowledgements

I would like to thank my supervisor Dr. Andreas Amann for his support and guidance throughout this project. His feedback and advice has been very appreciated and has made this an interesting and educational experience.

Contents

1 Introduction

1.1 Motivation

In the context of climate change and a growing human population, larger quantities of data than ever before, and powerful computers, ecological modelling and computer simulations are becoming increasingly important tools in the efforts to mitigate the effects of global warming, protect species from extinction and conserve the global food supply chain. Understanding and being able to form predictions about how ecological systems will react to shifts in the environment is essential for informing conservation policy in areas such as setting fishing quotas, establishing protected areas and choosing the least invasive strategies for developing agricultural landscape (13), (12). Also, when lacking a fundamental understanding of how ecosystems function, humans can unwittingly cause great damage to the natural world (20). With a global human population now predicted to reach 8.5 billion in 2030 (22), ensuring the persistence of food stocks is a major issue. As the climate becomes more volatile, the more understanding there is of the mechanisms behind ecological disasters such as pest-outbreaks, harmful algal blooms, and disease spreading (18) the better governing bodies will be able to prepare for the fallout of such events.

Phytoplankton is an especially interesting topic of study due to it's far-reaching influences. It is a significant primary producer and at the base of the aquatic food chain (11), so understanding the dynamics of phytoplankton populations can help form a basis for predictions about entire marine ecosystems (7). Phytoplankton blooms (red-tides) can lead to anaerobic conditions and dead zones (6) in the ocean or the release of toxins into the water (11) both which lead to the die-off of other marine life. Toxins released in harmful algal blooms (HABs) can also travel up the food-chain and affect human health (1). There has been considerable research into understanding the causes of red-tides but they are still not fully understood (20). Additionally, there is some scientific research going into the use of phytoplankton in bio-fuels (15),(4). All of this makes understanding the dynamics of phytoplankton populations especially topical and relevant and motivated it as the topic for this project.

1.2 Reaction Advection-Diffusion Equations

In the study of biodiversity it is often difficult and expensive to gather information about the distribution of various species, particularly in marine ecosystems (13)(20). Mathematical modelling offers a less expensive way to extrapolate what we do know about an ecological situation and draw useful conclusions.

Deterministic models, and in particular the branch of partial differential equations known as re-

action advection-diffusion equations like those studied in this project are useful in many ecological situations. They are used to simplify the dynamics of an ecological system to it's core elements and gain an understanding of the essential drivers of it's evolution. In the case of population dynamics, a reaction advection-diffusion equation reduces the complex list of factors which affect some population to it's patch size, production rate, death rate, and rates of spreading (advection and diffusion). Obviously this is a drastic oversimplification and insufficient to describe any real-life situation, however it would be impossible to account for all the interactions between species and climate that occur in a real ecosystem and a simple model can still be useful in a number of ways. Simple models can capture some of the fundamental mechanisms of a population's behaviour and allow us to gain a basic intuition for the relationship between various factors which can then be built upon. Also, if there exist sensible reasons for the occurrence of a certain phenomenon then these may also be applicable in the real world. Though most classical bifurcations in dynamical systems become degenerate with even small perturbations, saddle-node bifurcations and tipping points do exist in nature (20) and simplified models can help scientists understand at what values they may occur and form a basis for scientific predictions of the effects of environmental changes on biodiversity and populations of species.

1.3 The Equations

This project studies a deterministic model proposed by Jäger, C., Diehl, S. and Emans, M. (8), which consists of a set set of three coupled nonlinear partial differential equations and two differential equations that describe the vertical dynamics of phytoplankton in a one-dimensional column of freshwater. For this model, the z-axis is inverted and deeper depths correspond to greater z-values. The equations are as follows (8),

$$\frac{\partial A}{\partial t} = p(I,q)A - l_{bg}A - v\frac{\partial A}{\partial z} + d\frac{\partial^2 A}{\partial z^2} \tag{1a}$$

$$\frac{\partial R_b}{\partial t} = \rho(q,R_d)A - l_{bg}Rb - v\frac{\partial R_b}{\partial z} + d\frac{\partial^2 R_b}{\partial z^2} \tag{1b}$$

$$\frac{\partial R_d}{\partial t} = -\rho(q,R_d)A + l_{bg}Rb + d\frac{\partial^2 R_d}{\partial z^2} \tag{1c}$$

$$I(z) = I_0 exp - \left(\int_0^z kAdz + k_{bg}z\right) \tag{1d}$$

$$\frac{\partial R_s}{\partial t} = vR_b(z_{max}) - rR_s \tag{1e}$$

with functions p and ρ,

$$p(I,q) = \mu_{max}\left(\frac{q - q_{min}}{q}\right)\frac{I}{h + I} \tag{2a}$$

$$\rho(q,R_d) = \rho_{max}\left(\frac{q_{max} - q}{q_{max} - q_{min}}\right)\frac{R_d}{m + R_d} \tag{2b}$$

and,

$$q = \frac{R_b}{A} \tag{3}$$

Phytoplankton are photosynthesising organisms, they grow best in well-lit conditions with plenty of available nutrients (phosphorus in this case). At all depths algae will take in dissolved nutrients at a rate ρ, dependant on how many dissolved nutrients are available at that depth, $R_d(z)$, and how "well-fed" the algae already are. Once taken in, these nutrients are bound to the algae and hence they will move with identical dynamics. How "well-fed" algae are at a certain depth can be quantified by the ratio, q, between the concentrations of bound nutrients, R_b, and algae, A, present. In marine ecosystems, the euphotic zone is the shallow top layer of water where it is sufficiently bright to allow for photosynthesis (5). The growth of algae is hence limited to shallower water. The phytoplankton in this model are suspended in the water and not free-swimming so will sink helplessly out of the euphotic zone under the force of gravity at a rate v. They can only be transported back into this zone via turbulence, which is diffusing at a rate of d at all depths. This makes turbulence a significant factor in the dynamics of algal populations.

The equations here show algae and bound nutrients drifting and diffusing vertically in a one-dimensional column of water. The algal population grows with the photosynthesis-representing source term $p(I, q)$ and declines at a constant rate of respiration l_{bg}, which behaves as a sink term. It is assumed that the system is closed for nutrients R, which can exist in three states: bound to the algae, dissolved in the water and sedimented as R_s at z_{max}, the bottom of the water column. The state of these nutrients evolves in a cyclical fashion. Algae take up dissolved nutrients from the water at a rate ρ, changing R_d to R_b. When algae reach z_{max} it is assumed that the algae simply die, disappear from the system and their nutrients become sedimented as R_s. These sedimented nutrients then dissolve back into the water as R_d again at a rate r.
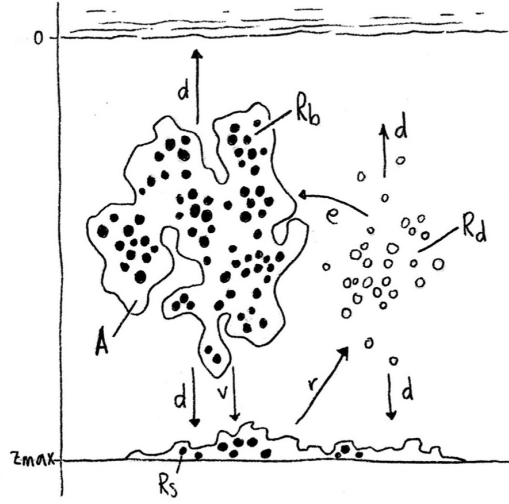
Figure 1: *Phytoplankton take in dissolved nutrients (white dots) at a rate ρ, converting them to particulate nutrients (black dots) bound in the phytoplankton. The bound nutrients diffuse up and down at a rate d and sink at a rate v with the phytoplankton cloud. When bound nutrients reach z_{max} they become sedimented as R_s. Sedimented nutrients are released back into the water column as dissolved nutrients at a rate r. The dissolved nutrients also diffuse up and down at a rate d but do not sink.*

The actual depth of the euphotic zone will depend on the concentration of phytoplankton present. Light intensity I will always decrease with depth as light is attenuated by background particles in the water at a rate k_{bg} but algae will also attenuate light at a rate k. Hence if there is a high concentration of algae at the surface it may be reasonable to assume that the euphotic zone will be limited to slightly shallower water.

6

Variable	Value	Definition
A		Algal carbon density $(mg\,C\,m^{-3})$
R_b		Concentration of particulate nutrients bound in algae $(mg\,P\,m^{-3})$
R_d		Concentration of dissolved nutrients $(mg\,P\,m^{-3})$
R_s		Pool of sedimented nutrients $(mg\,P\,m^{-2})$
I		Light intensity $(\mu mol\,photons\,m^{-2}\,s^{-1})$
I_0	300	Light intensity at the surface $(\mu mol\,photons\,m^{-2}\,s^{-1})$
d	0.01-1000	Turbulent-diffusion coefficient $(m^2\,day^{-1})$
v	0.25	Algal sinking velocity $(m\,day^{-1})$
l_{bg}	0.1	Specific algal maintenance respiration losses (day^{-1})
k	.0003	Specific light-attenuation coefficient of algal biomass $(m^2 mg\,C^{-1})$
k_{bg}	0.4	Background light-attenuation coefficient (m^{-11})
μ_{max}	1.2	Maximum specific algal production rate (day^{-1})
q_{min}	0.004	Maximum algal nutrient quota $(mg\,P\,mg\,C^{-1})$
q_{max}	0.04	Minimum algal nutrient quota $(mg\,P\,mg\,C^{-1})$
h	120	Half-saturation constant of light-dependant algal production $(\mu mol\,photons\,m^{-2}\,s^{-1})$
ρ_{max}	0.2	Maximum specific algal nutrient uptake rate $(mg\,P\,mg\,C^{-1}\,day^{-1})$
m	1.5	Half-saturation constant of algal nutrient uptake $(mg\,P\,m^{-3})$
r	.02	Specific mineralisation rate of sedimented nutrients (day^{-1})

Table 1: Table of variables used, taken from Jäger et al. (8)

1.4 Model Simplification

The model in (8) is of course a huge simplification of the true dynamics of phytoplankton in an aquatic environment. It is assumed that the only direct limiting factors to algal growth are light and phosphorus availability. Algae and a single nutrient are isolated from all other elements of a marine ecosystem such as alternative nutrients like nitrogen and silicate (11), predation by organisms of higher trophic levels, and competition with other organisms for nutrients. Light intensity is uniform and not adjusted to reflect day and night or seasonal variation and diffusion and sinking coefficients are not only constant in time but also in depth. This is unrealistic as it does not account for the increased turbulence that occurs near the surface of bodies of water (10). The model is 1-dimensional so changing depths on the lake floor are not accounted for and this may have considerable impact on the behaviour of the system.

Nonetheless, this model can educate us on the basic behaviour of algae and form a blueprint for further study upon which more models that account for more of the ecosystem's true complexity

can be built. There is a possibility that mechanisms discovered in this simple model will translate and still be relevant in more complex models and perhaps uncover fundamental truths about the drivers of a population of phytoplankton's dynamics.

1.5 Boundary Conditions

The same boundary conditions as provided in the paper (8) are used in this project and these are shown in table 2 below.

Algae, particulate and dissolved nutrients can neither enter nor leave the water column at the surface. To establish this, Robin and Neumann boundary conditions are set such that the convective flux for all three variables is zero. As the dynamics of A and R_b are governed by both drift and diffusion and those of R_d by diffusion alone, their net currents can be described as,

$$J_A = vA - dA'$$
$$J_{R_b} = vR_b - dR_b'$$
$$J_{R_d} = -dR_d'.$$

Setting J_A, J_{R_b} and J_{R_d} to zero at the surface yields the boundary conditions provided in table 2.

When algae reach z_{max} they are assumed to sink out of the system, the particulate nutrients which are bound to them then become part of the sediment R_s. This means that at $z = z_{max}$ there is no diffusion of algae and bound nutrients and their net current is a downward drifting current only, i.e. only the drift current may contribute to the settling of particulate nutrients at z_{max}. To achieve this, Neumann boundary conditions are used which set the diffusive element of the current dA', dR_b' to zero, giving rise to the conditions in table 2. The Robin boundary condition for R_s and R_d then preserves the concentration of nutrients in the system by ensuring the influx current of nutrients into R_s from R_d via diffusion d is equal to the outflux by remineralisation r, $J_{R_d} = -dR_d' = -rR_s$.

Neumann conditions at $z = 0$ and $z = z_{max}$ also indicate that minima and maxima must occur for A and R_b at z_{max} and for R_d at the surface. This can be seen relatively clearly in figure 6 for turbulence values $d = 0.1, 1.0$ where the z_{max} shifts from behaving as a maximum in shallow water columns, to behaving as a minimum in deeper water columns. This is less clear for water with turbulence $d = 100$ so it is illustrated in the appendix in figure A2 where the line plots are all achieving minima at z_{max} for A, maxima at z_{max} for R_b and minima at the surface for R_d.

Note: If the sediment layer is kept constant at zero then $vR_b = rR_s$ leading to the boundary condition in column z_{max} (i), allowing us to perform calculations without R_s.

Variable	Surface	z_{max} (i)	z_{max} (ii)
A	$vA(0) - dA'(0) = 0$	$A'(z_{max}) = 0$	$A'(z_{max}) = 0$
R_b	$vR_b(0) - dR_b'(0) = 0$	$R_b'(z_{max}) = 0$	$R_b'(z_{max}) = 0$
R_d	$R_d'(0) = 0$	$dR_d'(z_{max}) - vR_b(z_{max}) = 0$	$rR_s - dR_d'(z_{max}) = 0$
I	$I(0) = I_0$		

Table 2: Boundary conditions, taken from Jäger et al. (8)

1.6 Variables of Interest

There are plenty of potential areas for exploration in this model. Studying the effect of the total amount of nutrients in the system $R = R_d + R_b$ would inform us about at which levels we can expect eutrophication and algal blooms to occur and for what duration we can expect them to last. We could explore the effects of murkier water by increasing the background light attenuation coefficient k_{bg} or look at how the model changes for algae with higher densities by increasing the sinking velocity v. One of the most interesting variables in the model is the turbulence coefficient d, whose effect is not immediately obvious yet plays a vital role in the survival of phytoplankton populations.

As light is needed for algal growth, the majority of production will occur in the euphotic zone of the water column, where $I(z)$ is large. As the algae in this model do not have the ability of self-propulsion and have a higher density than water they will sink out of this zone at a rate v, along with the nutrients that are bound to them. Only turbulence can then transport them back into a depth where production can take place. Otherwise they will die out at a rate $l_{bg}A$ near z_{max} where it is very dark and photosynthesis cannot occur, or else enter the sediment and sink out of the system (8).

Hence, the variables of focus for this project are d, the degree of turbulence in the water, and I_0 the light intensity at the surface and the intention is to develop a thorough understanding of the mechanism by which these variables will affect the rest of the system.

This project aims to reproduce the results of Jäger et al. (8) in the water column depth-turbulence space and examine changes caused by shifts in d and I_0.

2 Method

2.1 Initial Approach

To find equilibrium solutions for the system the initial (unsuccessful) approach used set all partial time derivatives to zero and attempted to solve the newly created system of first order ordinary differential equations. This was attempted via the shooting method (19). By defining $A_2 = A'$, $R_{b2} = R_b'$ and $R_{d2} = R_d'$ as new variables with $A' = \frac{\partial A}{\partial z}$, the system was reduced to the first-order system given below,

$$A_1' = A_2$$
$$A_2' = \frac{1}{d}\left(vA_2 - p(I,q)A_1 + l_{bg}A_1\right)$$
$$R_{b1}' = R_{b2}$$
$$R_{b2}' = \frac{1}{d}\left(vR_{b2} - \rho(q,R_{d1})A_1 + l_{bg}R_{b1}\right)$$
$$R_{d1}' = R_{d2}$$
$$R_{d2}' = \frac{1}{d}\left(\rho(q,R_{d1})A_1 - l_{bg}R_{b1}\right)$$
$$I' = -(kA_1 + k_{bg}z)I$$

with boundary conditions,

$$vA_1(0) - dA_2(0) = 0 \qquad\qquad A_2(z_{max}) = 0$$
$$vR_{b1}(0) - dR_{b2}(0) = 0 \qquad\qquad R_{b2}(z_{max}) = 0$$
$$R_{d2}(0) = 0 \qquad\qquad dR_{d2}(z_{max}) - vR_{b1}(z_{max}) = 0$$
$$I(0) = I_0$$

Taking the initial homogeneous conditions for $A_1 = 300$, $R_{b1} = 2.2$, $R_d = 30$ and $I = 300$ (8) as known, the remaining values for A_2, R_{b2} and R_{d2} were guessed and a fourth-order Runge-Kutta method (19) was used to interpolate the initial value problem to z_{max}. The predicted values for A_2, R_{b2} and R_{d2} and $dR_{d2} - vR_{b1}$ would be compared to the given boundary conditions. The intention was to treat the differences between predicted and given boundary conditions as an equation in $A_2(0), R_{b2}(0)$ and $R_{d2}(0)$ and solve for it's roots using the root function from the SciPy optimize module (9).

The values at z_{max} obtained via Runge-Kutta iteration displayed very high sensitivity to initial conditions and the majority of chosen initial conditions led to the solution blowing up. Hence any shooting method implementations failed to converge. This suggested that the system may be a stiff system (3). To allow for this possibility a different approach was taken: the finite difference method

was used to calculate solutions for subsequent time steps over a long period of time until the system began to settle into a stable, stationary distribution.

2.2 The Finite Difference Method

To achieve the results shown in the rest of this project an explicit finite difference method was used to obtain numerical approximations of the differential equations 1a-1e. The first-order time derivative was approximated by the forward Euler method and the first and second-order space derivatives were approximated by first and second-order central difference equations (19). This yielded,

$$A_z^{t+\Delta t} = A_z^t + \Delta t \left(p(I_z^t, q_z^t) A_z^t - l_{bg} A_z^t - v \frac{A_{z+\Delta z}^t - A_{z-\Delta z}^t}{2\Delta z} + d \frac{A_{z+\Delta z}^t - 2A_z^t + A_{z-\Delta z}^t}{\Delta z^2} \right) \tag{4}$$

$$R_{bz}^{t+\Delta t} = R_{bz}^t + \Delta t \left(\rho(q_z^t, R_{dz}^t) A_z^t - l_{bg} R_{bz}^t - v \frac{R_{bz+\Delta z}^t - R_{bz-\Delta z}^t}{2\Delta z} + d \frac{R_{bz+\Delta z}^t - 2R_{bz}^t + R_{bz-\Delta z}^t}{\Delta z^2} \right) \tag{5}$$

$$R_{dz}^{t+\Delta t} = R_{dz}^t + \Delta t \left(-\rho(q_z^t, R_{dz}^t) A_z^t + l_{bg} R_{bz}^t + d \frac{R_{dz+\Delta z}^t - 2R_{dz}^t + R_{dz-\Delta z}^t}{\Delta z^2} \right) \tag{6}$$

$$R_s^{t+\Delta t} = R_s^t + \Delta t \left(v R_{bz_{max}}^t - r R_s^t \right) \tag{7}$$

and equation 1d for I is discretized by expressing $\int_0^z kA dz$ as $\sum_i kA(i)\Delta z$ where $i = 0, \Delta z, 2\Delta z, ..., z$.

2.3 Discretising Boundary Conditions

To discretise the boundary conditions in table 2 the second-order formula for the first derivative, $f'(x) = \frac{1}{2h} \left(-3f(x) + 4f(x + h) - f(x + 2h) \right) + O(h^2)$ is used (19).
In the case of Neumann boundaries where f'(x) = 0 this simplifies to,

$$-3f(0) + 4f(1) - f(2) = 0$$
$$-f(M - 2) + 4f(M - 1) - 3f(M) = 0$$

which give us,

$$R_{d0} = \frac{1}{3}(4R_{d1} - R_{d2})$$

11

for the boundary condition for R_d at the surface. To obtain a second order discretisation of the Robin boundary conditions at the surface,

$$0 = vA_0 - \frac{d}{2\Delta z}(-3A_0 + 4A_1 - A_2)$$

$$\implies A_0 = \frac{d}{2v\Delta z + 3d}(4A_1 - A_2)$$

and,

$$R_{b0} = \frac{d}{2v\Delta z + 3d}(4R_{b1} - R_{b2}).$$

Similarly at z_{max} with $M = z_{max}$,

$$A_M = \frac{1}{3}(-A_{M-2} + 4A_{M-1})$$

$$R_{bM} = \frac{1}{3}(-R_{bM-2} + 4R_{bM-1}).$$

For the Robin condition,

$$0 = rR_s - \left(-\frac{d}{2\Delta z}(-3R_{dM} + 4R_{dM-1} - 3R_{dM-2})\right)$$

$$\implies R_{dM} = \frac{1}{3d}(4dR_{dM-1} - dR_{dM-2} + 2r\Delta zR_s).$$

These results are summarised in table 3.

Variable	Surface	z_{max}
A	$A_0 = \frac{d}{2v\Delta z + 3d}(4A_1 - A_2)$	$A_M = \frac{1}{3}(-A_{M-2} + 4A_{M-1})$
R_b	$R_{b0} = \frac{d}{2v\Delta z + 3d}(4R_{b1} - R_{b2})$	$R_{bM} = \frac{1}{3}(-R_{bM-2} + 4R_{bM-1})$
R_d	$R_{d0} = \frac{1}{3}(4R_{d1} - R_{d2})$	$R_{dM} = \frac{1}{3d}(4dR_{dM-1} - dR_{dM-2} + 2r\Delta zR_s)$
I	$I(0) = I_0$	

Table 3: Discretised boundary conditions

2.4   Building Up to a Solution

The final solution was built up to in a step-by-step fashion to ensure sure everything was working as expected. Figure 2 shows three of these steps. First the equations for A were simplified to drift-diffusion only equations and these were approximated by the finite difference method. An initial concentration with a 'bump' a quarter of the way down the water column was considered and this bump can be seen sinking down the water column and diffusing from areas of higher concentration to areas of lower concentration. The total concentration of A is conserved here. When the l_{bg}-term was added this bump shrinks dramatically and the overall concentration of A is reduced. When the p function is finally included the concentration increases. The effect of these terms can be emphasised by tweaking v,d and l_{bg} accordingly.
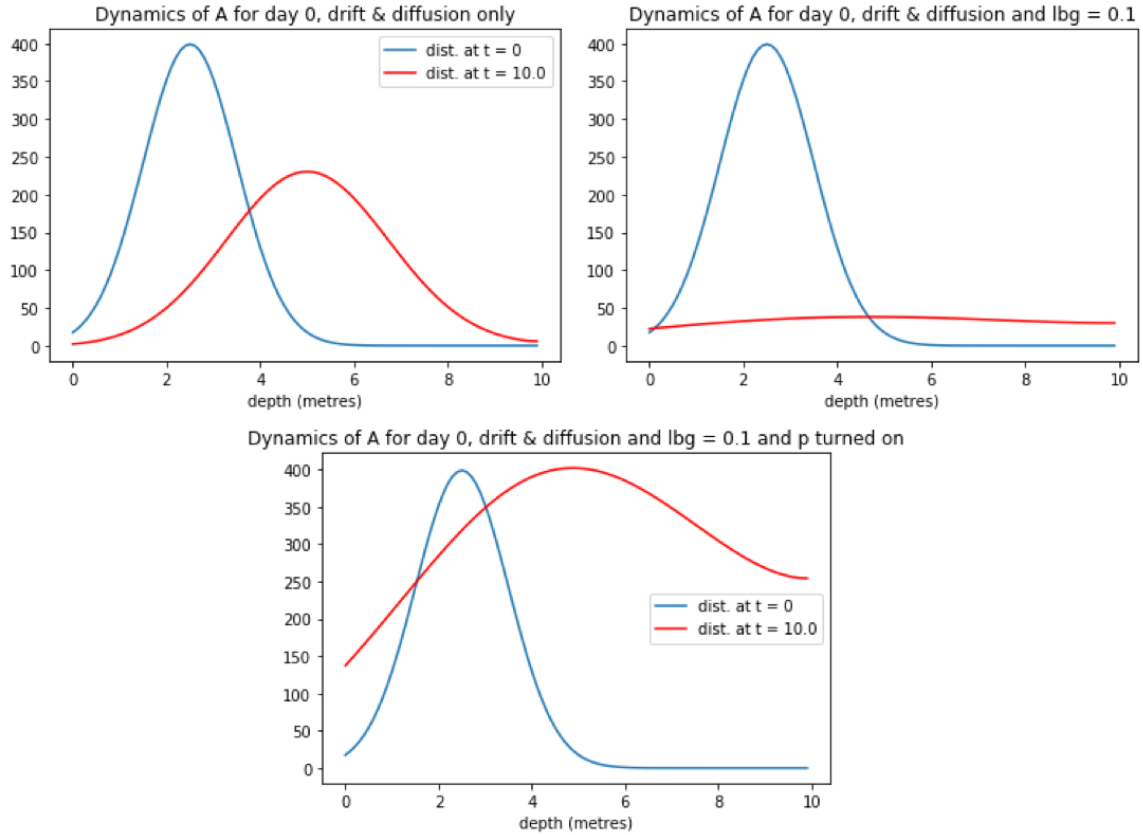
Figure 2: *Some of the steps in building up to the full model 1. First a model of just drift and diffusion was created, then the loss term l_{bg} was added, followed by the production term p*

2.5 Finding the Stationary Distribution

To find the stationary distribution of the concentration of phytoplankton and nutrients in the water column the finite difference method was used to calculate consecutive steps until the system stopped changing with time. The time at which the solution settled into a stationary distribution varied depending on the values of turbulence d and water column depth z_{max}. This was easiest to visualize using 3-dimensional surface plots. Figure 3 shows that for $d = 0.1$ and $z_{max} = 30$ the solution doesn't reach it's stationary distribution until around 800 days but in figure 4 the solution with $d = 10$ and $z_{max} = 10$ settles in under 200 days. For low values of d like in figure 3 the solution oscillated around it's stationary distribution before it settled into it and this behaviour was further exaggerated with deeper water column depths. More of these time-evolution plots are given in figure A1 in the appendix. Table 4 shows how long it took solutions to settle into a stationary distribution for different combinations of (z_{max},d)-pairs.

	$z_{max} = 10$	$z_{max} = 30$
$d = 0.1$	400	> 800
$d = 1$	< 200	< 300
$d = 10$	< 200	< 200
$d = 100$	200	300

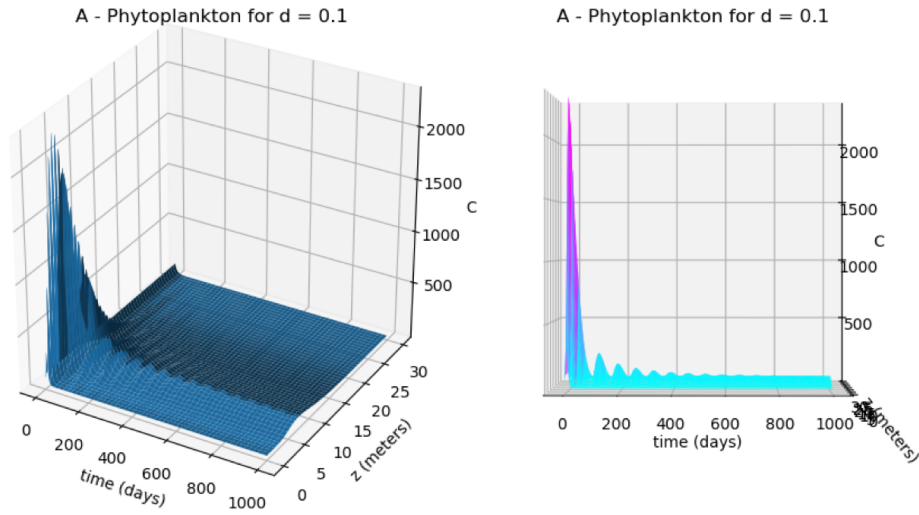Table 4: *The number of days before solution became stationary for (d,z_{max})-pairs.*

Figure 3: *Surface plots showing the evolution of phytoplankton concentrations over time for $z_{max} = 30$ and $d = 0.1$. The system reaches a stationary distribution around day 800.*

14
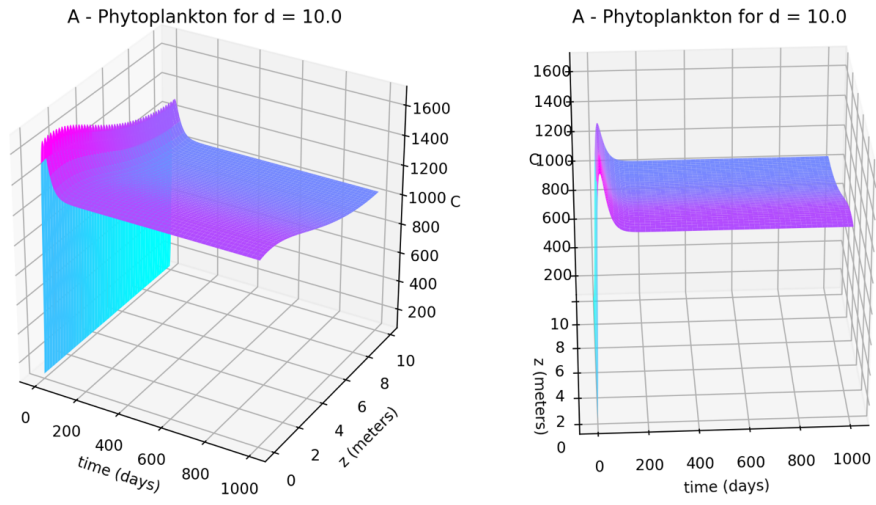
Figure 4: *Surface plots showing the evolution of phytoplankton concentrations over time for $z_{max} = 10$ and $d = 10.0$. The system reaches it's stationary distribution before day 200.*

3 Results

3.1 Reproducing the Depth-Turbulence Plots

The first aim of this project was to reproduce the heatmaps of the first two rows of figure 5 which was taken from the paper being studied (8). The first row here shows concentrations of phytoplankton at different depths z (z-axis), for different water column depths z_{max} (x-axis), for five different turbulence values $d = \{0.1, 1, 10, 100, 1000\}$. The second row shows the same for total nutrient concentration $R = R_d + R_b$. Being able to reproduce these heatmaps would both verify the accuracy of the work by Jäger et al.(8) and ensure the finite difference method used here is calculated correctly and that any conclusions drawn from it's implementation are reliable.

As this method was quite computationally intensive a step size of $\Delta z = 0.1$ with a corresponding time step of $\Delta t = \frac{\Delta z}{1000}$ was chosen instead of $\Delta z = 0.02$ as used in (8). Stationary distributions were calculated thirty times for water columns of depth $0 - 30$ instead of $0 - 50$ and this is taken as sufficient to conclude that the approximations agree. The value of $d = 1000$ was also omitted. For $d = 100$ a smaller timestep ratio of $\Delta t = \frac{\Delta z}{2000}$ was required for stability and a corresponding slightly larger spacial step $\Delta z = 0.2$ was used in order to keep the simulation running reasonably fast.

The number of finite difference steps needed to reach a stationary distribution varied for each value of d and these figures are shown in days in table 4. For each d value the simulation was run for the number of days needed for the $z_{max} = 30$ water column to reach a stationary distribution. In the case of $d = 0.1$ the simulation was only run until day 600 in order to save time, it can be seen in figure 3 that this is still reasonably close to the true stationary distribution of A.
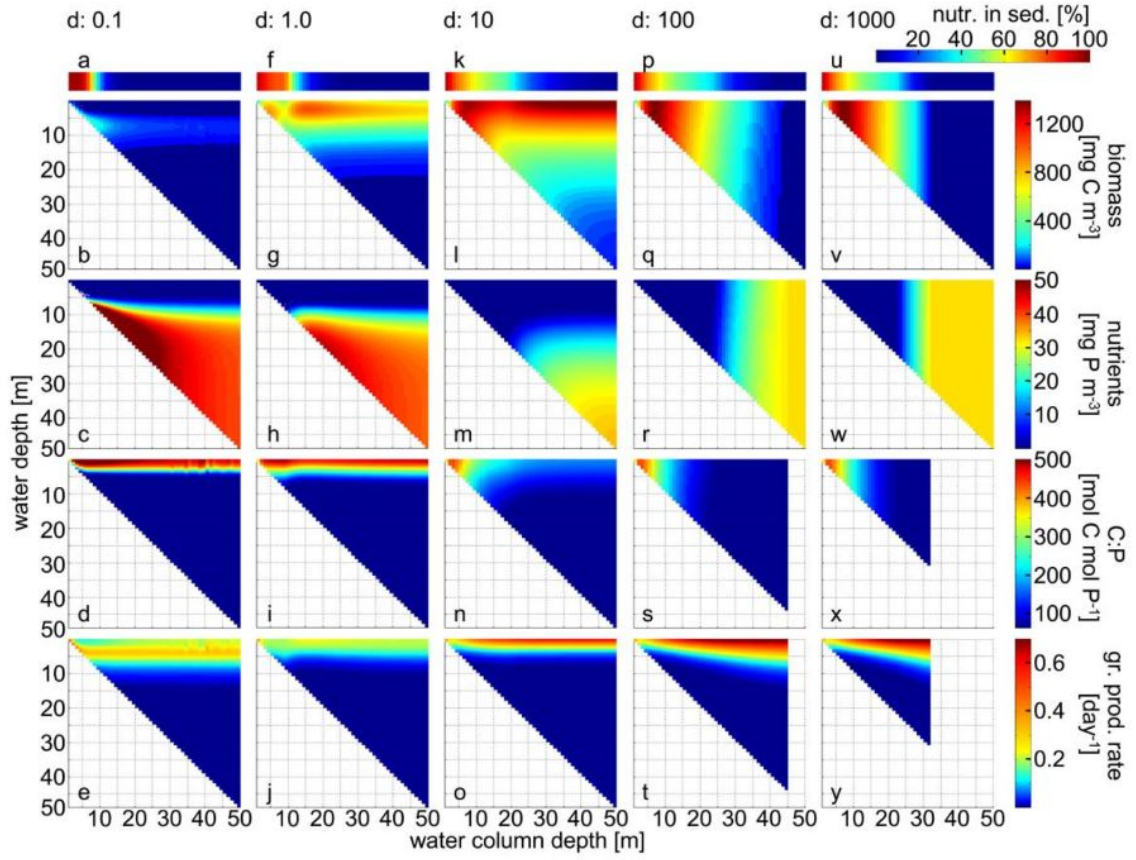
Figure 5: *Stationary distributions of phytoplankton and nutrient concentrations for different turbulence values in the water column depth-depth space, from (8)*
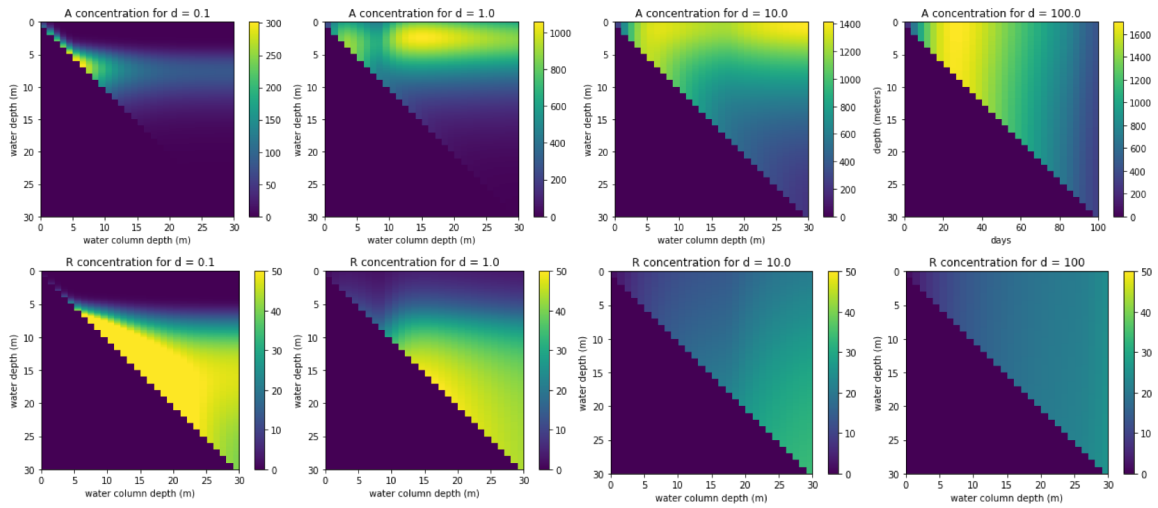
Figure 6: *Stationary distributions of phytoplankton and nutrient concentrations for different turbulence values in the water column depth-depth space approximated by the finite difference method*

3.2 Stationary Distributions for Various Turbulence Values

In order to form a clearer picture of how direct changes in d affect algal distributions a plot of the stationary distribution changing with d for a fixed water column depth is useful. Figures 7 and 8 show the stationary distributions of A and R_b for values of d ranging from $0-10$. Very small values of d, in the range $0-0.5$ do not appear sufficient to sustain an algal population for a water column of depth 15 metres, suggesting that there is not enough turbulence bringing algae back into the euphotic zone to sustain life.

The distributions of A and R_b show striking peaks when d lies between 2 and 4, with R_b peaking below A in the water. This demonstrates a complex interplay between different factors: a high production rate p near the surface causes algal populations to bloom, leading to insufficient dissolved nutrients and a large number of algae with a low nutrient quota q. When these algae with low q sink, the value of R_d increases while A decreases at a rate $l_{bg}A$ creating optimal conditions (high R_d, low q) for a high nutrient uptake function ρ which then leads to an increase in R_b. Turbulence blurs this effect as d increases but it is not quite clear why the peak in R_b's concentration sinks with increasing d.

For d greater than 6 the water column is well-mixed with more algae being produced at the surface and dissolved nutrients being reintroduced to the water via remineralisation and respiration losses at deeper depths. This creates the two opposing gradients visible for $d > 6$ in 7 and 8.
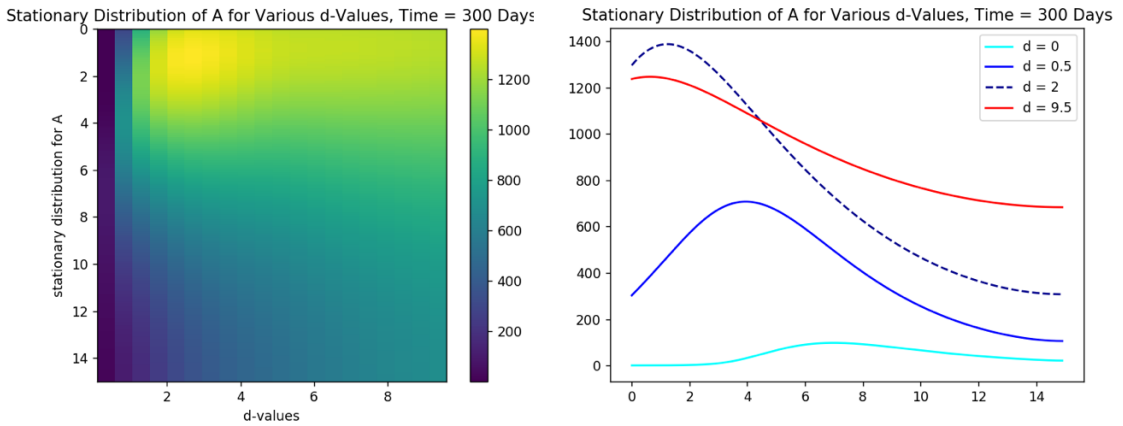

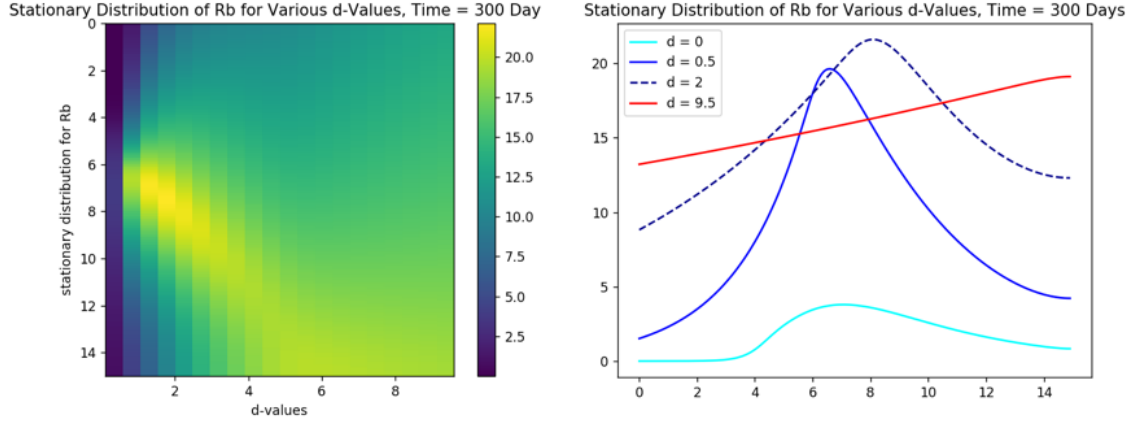Figure 7: *Stationary distributions of A for $d \in [0, 10]$*

18

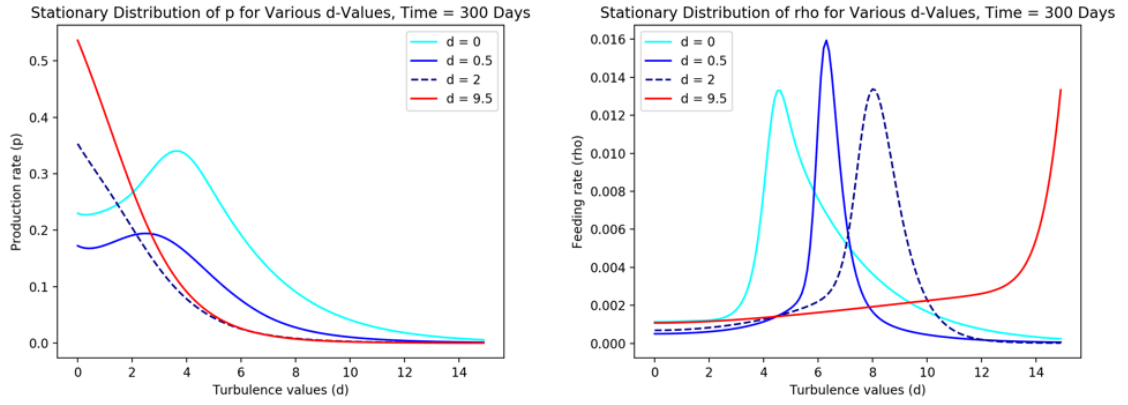Figure 8: *Stationary distributions of R_b for $d \in [0, 10]$*

Figure 9: *The distributions of the production rate p and nutrient uptake rate ρ.*
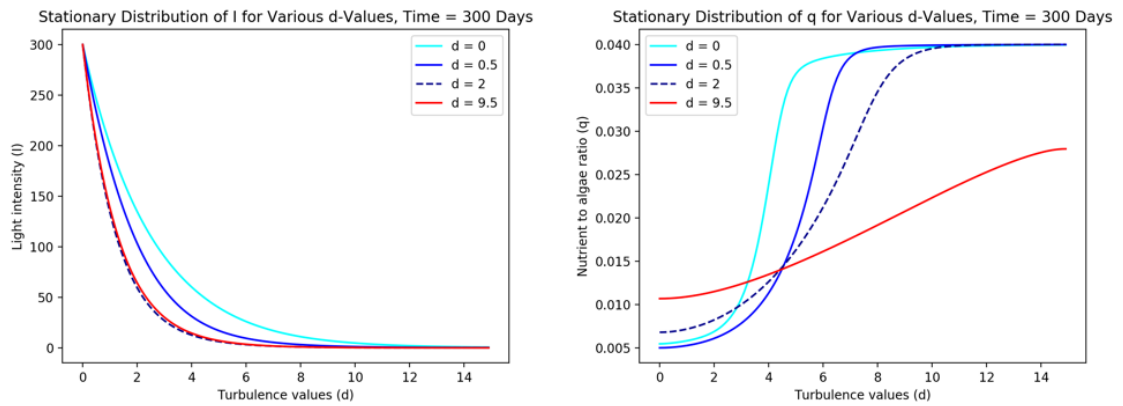

19

Figure 10: *The distributions of light intensity I and algal nutrient quota q.*

3.3   Light Shifts

To explore the impact of light intensity on this model a number of simulations were run on a water column of depth $z_{max} = 30$. In the heatmap on the left of figure 11 the light intensity at the surface was doubled to $600\,\mu\,mol\,photons\,m^{-2}\,s^{-1}$ at $t = 60$ days and the solution quickly moves to a new stationary distribution of almost double the concentration. The heatmap on the right-hand side of figure 11 displays the an almost equal and opposite effect when the light intensity at the surface was halved to $150\,\mu\,mol\,photons\,m^{-2}\,s^{-1}$. The heatmaps in figure 11 show arcing fronts as phytoplankton at the surface are affected first and this change then spreads to deeper depths over time.
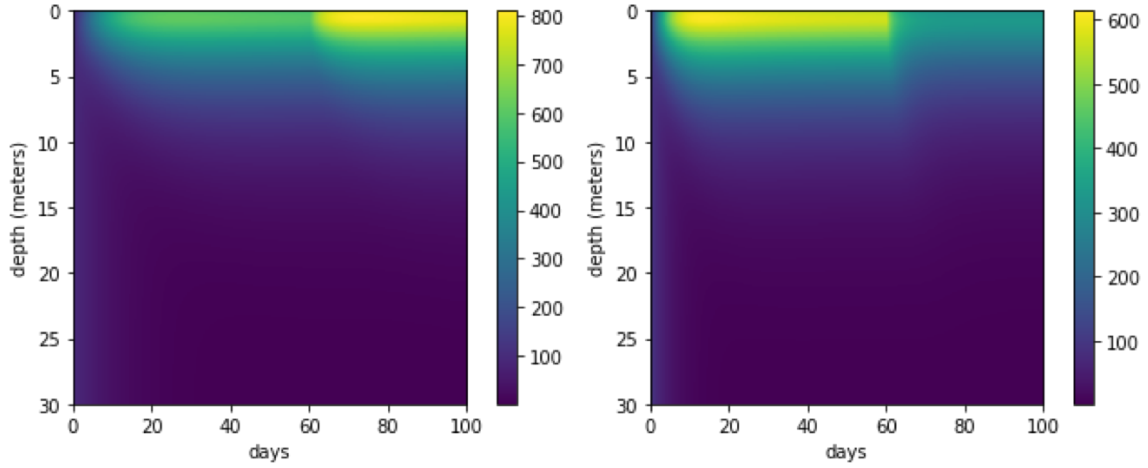
Figure 11: *The heatmap of the left shows the effect of light intensity doubling from 300 to 600 on the 60th day. The heatmap on the right shows the effect of light intensity being halved on the 60th day.*

Next, the scenario of a period of total darkness, where there was no light at all for a number of days, was considered. The intention was to see how the phytoplankton populations would react and if, and how quickly, they would recover. This would be applicable in situations of an extreme climate event, such as a Tambora volcanic eruption in 1815 where a distance of 600km was thrown into darkness for two days (21) or an oil spill, where the surface of the sea in any areas of water coated in oil would obviously be obscured from sunlight.

Simulations were run for various turbulence levels over 500 days on water columns of depth 20m and a 10 day period of darkness occurred on the 250th day. Figure 12 shows results for $d = 5$.

Figures for $d = 1, 10$ and 100 can be seen in the appendix, figures A3, A4 and A5 . These figures show concentrations recover quickly from periods without light and even increase a little beyond the stationary distribution for a short time before settling back to the original stationary distribution.
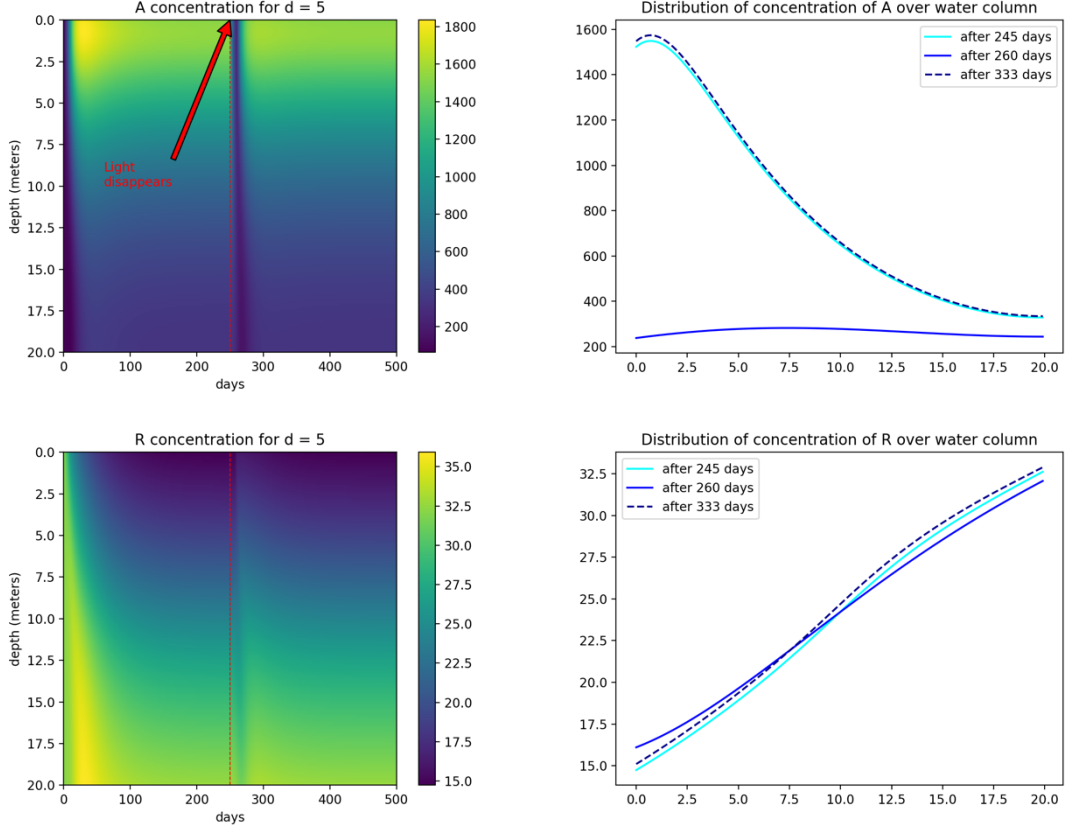

Figure 12: *Light disappears for 10 days on the 250th day, indicated by the red dashed line. Conditions are d=5, z_{max}=20m. Algal populations drop to a lower, more homogeneous distribution of A $\approx$ $200\,mg\,P\,m^{-3}$ while light is absent but make a full recovery within 100 days of light returning. In fact, the population slightly surpasses the stationary distribution for a brief period of time after the light returns.*

3.4   Study of a Particular Water Column

In order to gain a more thorough understanding of the mechanism by which phytoplankton populations respond to light changes, the water column with $d = 1.0$ and depth $z_{max} = 20$ is given special attention. This column is worth studying because, as can be seen in figure 6, the phytoplankton displays non-trivial peak in it's stationary distribution for this (d, z_{max})-pair. The simulation was run for 1000 days to ensure there was sufficient time for a stationary distribution to be reached

before and after the light disappearance, which lasted for 100 days on the 500th day. Heatmaps of the phytoplankton and nutrient distributions over the 1000 days are shown in figure 13.

The mechanics by which the population originally grows become more apparent in figure 14 which enlarges the first 100 days in the water column. Nutrients initially have a homogeneous distribution throughout the water and phytoplankton populations bloom due to the high availability of nutrients in the euphotic zone. However as nutrients become bound in the algae they sink with it and by day 18 the bulk of the nutrients are gathered around 7m below the surface. This peak concentration of nutrients moves slowly down until the distribution in R-concentration resembles a smooth positive gradient from 0 to z_{max}. This process behaves as as a natural brake on phytoplankton blooms near the surface.
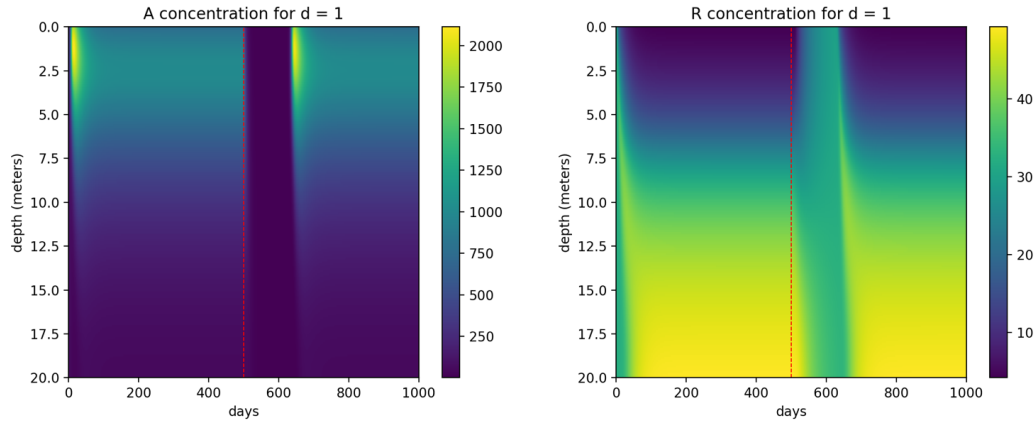

Figure 13: *Heatmaps showing the evolution of phytoplankton and nutrient distributions with time. Light disappears for 100 days on the 500th day, marked with a red dashed line*
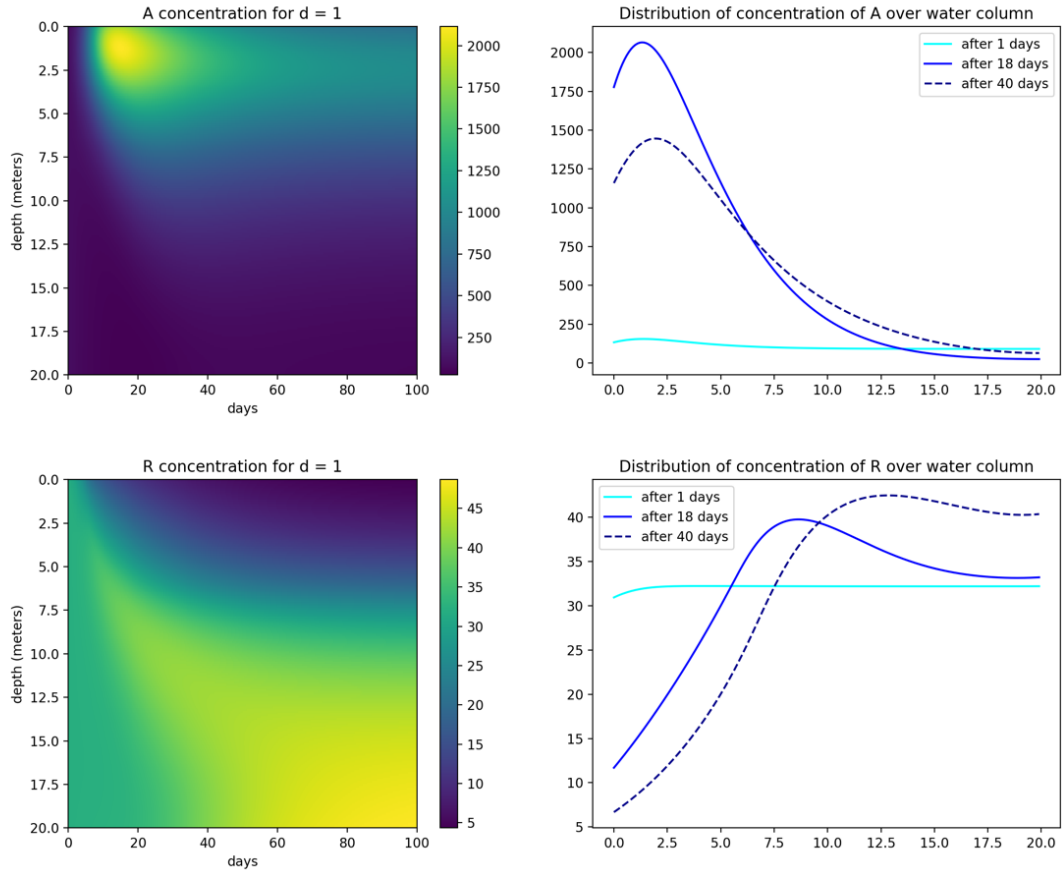
Figure 14: *Heatmaps showing the evolution of phytoplankton and nutrient distributions for the first 100 days.*

Figure 15 zooms in on the moment when light disappears from the surface. The phytoplankton population quickly starts diminishing and it drifts and diffuses downwards. As this happens the nutrient spread becomes more homogeneous again.
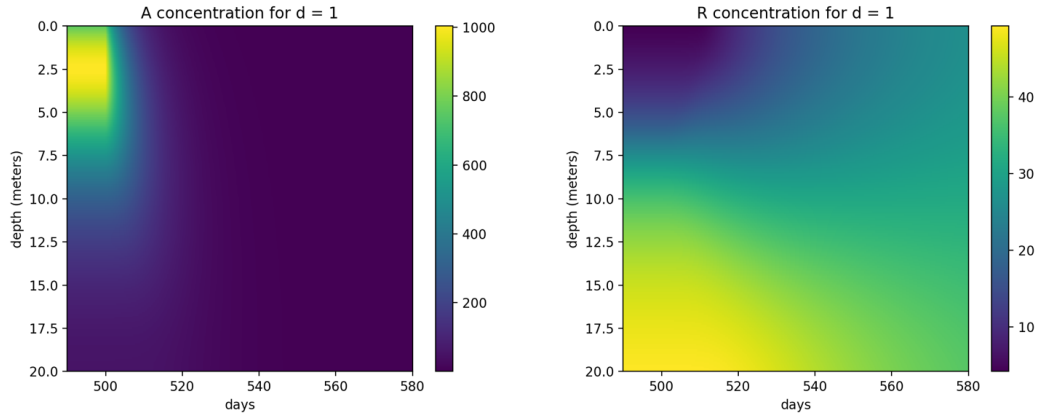
Figure 15: *Enlargement of the days when light first disappears*

Figure 16 is surprising because it shows that extremely little algae needs to be present in the system for the population to recover once conditions improve. On day 600 the maximum concentration of A in the water column is around $0.007\ mg\,P\,m^{-3}$ but 40 days later the distribution has a peak near $1750\ mg\,P\,m^{-3}$. This suggests that the peaked stationary distribution of A is almost globally stable for $A \neq 0$.
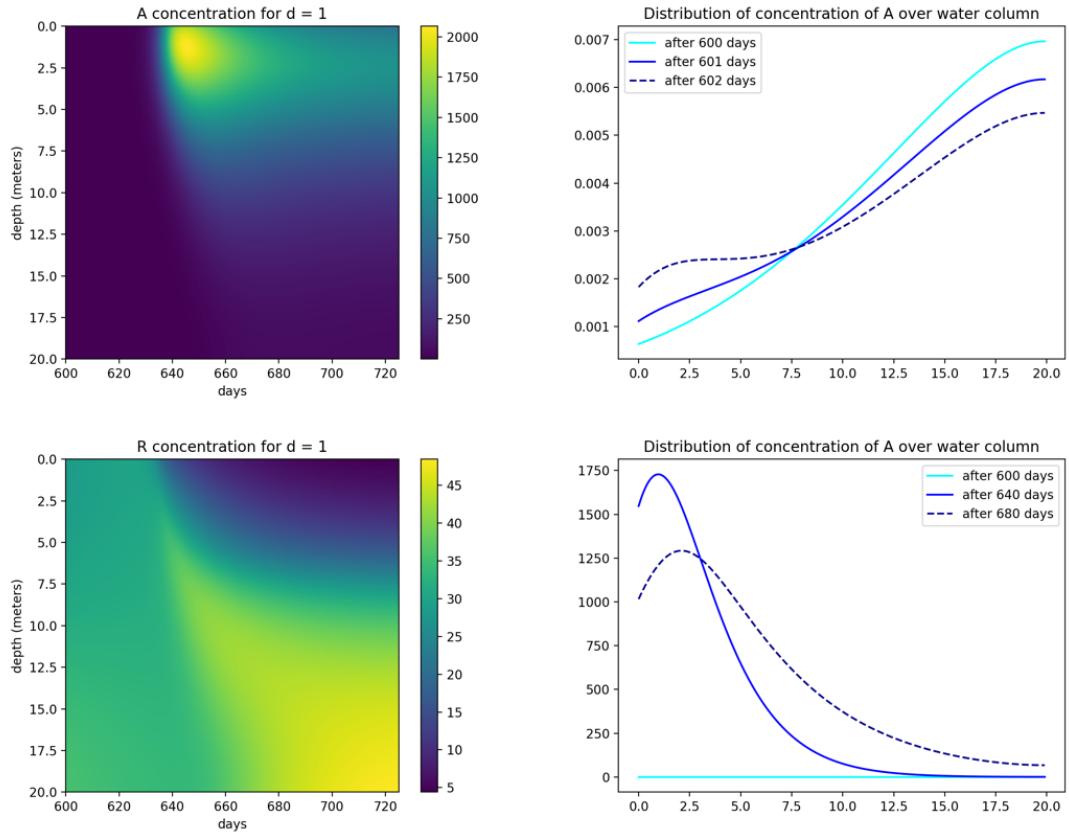
Figure 16: *Enlargement of the days when light returns to normal.*

Population blooms are observed in both figures 14 and 16. These show how, in this model, any small phytoplankton population can lead to a population explosion due to the availability of nutrients near the surface, which support a high rate of photosynthesis. It is natural to expect an algal population to decrease once light is reduced, as photosynthesis cannot take place, but it is interesting to note that if light conditions return then a population bloom can usually be expected before the algae settles back into it's stationary distribution. This is a nice example of the resilient and self-regulating nature of ecosystems.

4   Discussion

In this project an explicit finite difference method was used to approximate the deterministic model provided by Jäger et al. in (8). This approximation was successful in replicating the results in the depth-turbulence space originally produced in (8) and extended the exploration of how changes in light intensity affect a phytoplankton distribution by generating a number of simulations. It was found that the stationary distributions of these populations are very stable for a fixed set of parameters and that even extremely low initial concentrations of algae are capable of creating large population blooms, provided conditions are favourable.

Since phytoplankton form the foundation of much of marine life (11), this is a comforting reminder of the resilience of nature. This model is, however, fundamentally wrong in that it fails to account for the innumerable other processes which play a role in the survival of a phytoplankton species. Any conclusions formed by it would need to be verified through much practical research and experimentation. This model does still have some purpose in that it captures some of the fundamental mechanisms by which algal populations survive and can serve as a basic aide to understanding from which more sophisticated models can be built.

References

[1] Bennett, J., Dolin, R. and Blaser, M. (2015). *Mandell, Douglas, and Bennett's principles and practice of infectious diseases* (8th ed.). Elsevier Saunders, p.3192.

[2] Bouman, B. (1992). *Linking physical remote sensing models with crop growth simulation models, applied for sugar beet.* International Journal of Remote Sensing, p.2565-2581.

[3] Burden, R. and Faires, J. (2011). *Numerical analysis* (9th ed.). Boston, MA: Brooks/Cole, Cengage Learning, p.348.

[4] Coons, R. (2018). *Danish researchers look to harness bioluminescent algae to light cities.* [online] Available at: `http://biofuelsdigest.com/nuudigest/2018/05/07/danish-researchers-look-to-harness-bioluminescent-algae-to-light-cities/`

[5] Encyclopedia Britannica. (2020). *Euphotic zone — oceanography.* [online] Available at: `https://www.britannica.com/science/euphotic-zone`.

[6] US EPA. (n.d.). *The Effects: Dead Zones and Harmful Algal Blooms — US EPA.* [online] Available at: `https://www.epa.gov/nutrientpollution/effects-dead-zones-and-harmful-algal-blooms`

[7] Jäger, C., Diehl, S., Matauschek, C., Klausmeier, C. and Stibor, H. (2008). *Transient Dynamics of Pelagic Producer-Grazer Systems in a Gradient of Nutrients and Mixing Depths.* Ecology, p.1272-1286

[8] Jäger, C., Diehl, S. and Emans, M. (2010). *Physical Determinants of Phytoplankton Production, Algal Stoichiometry, and Vertical Nutrient Fluxes.* The American Naturalist, p.E91-E104

[9] Jones, E. et al. (2001). *SciPy: Open source scientific tools for Python.* Available at: `http://www.scipy.org/`

[10] Kirillin, G. , Shatwell, T. (2016) *Generalized scaling of seasonal thermal stratification in lakes.* Earth-Science Reviews, p.180

[11] Lindsey, R. and Scott, M. (2010). *What are Phytoplankton?.* [online] Available at: `https://earthobservatory.nasa.gov/features/Phytoplankton`

[12] Lucey, J., Palmer, G., Yeong, K., Edwards, D., Senior, M., Scriven, S., Reynolds, G. and Hill, J. (2017). *Reframing the evidence base for policy-relevance to increase impact: a case study on forest fragmentation in the oil palm sector.* Journal of Applied Ecology, p.731-736.

[13] McClellan, C., Brereton, T., Dell'Amico, F., Johns, D., Cucknell, A., Patrick, S., Penrose, R., Ridoux, V., Solandt, J., Stephan, E., Votier, S., Williams, R. and Godley, B. (2014). *Understanding the Distribution of Marine Megafauna in the English Channel Region: Identifying Key Habitats for Conservation within the Busiest Seaway on Earth.* PLoS ONE, p.e89720.

[14] McKinney, W. others, (2010.) *Data structures for statistical computing in python.* In Proceedings of the 9th Python in Science Conference. p. 51–56.

[15] Narwani, A., Lashaway, A., Hietala, D., Savage, P. and Cardinale, B. (2016). *Power of Plankton: Effects of Algal Biodiversity on Biocrude Production and Stability.* Environmental Science Technology, p.13142-13150.

[16] Oliphant, T.E. (2006). *A guide to NumPy,.* Trelgol Publishing USA.

[17] Petrovskii, S. V., Malchow, H. (2009). *Mathematical Models of Marine Ecosystems.* Oxford, UK: EOLSS.

[18] Rivers-Moore, N., Hughes, D. and de Moor, F. (2008). *A model to predict outbreak periods of the pest blackfly Simulium chutteri Lewis (simuliidae, Diptera) in the Great Fish River, Eastern Cape province, South Africa.* River Research and Applications, p.132-147.

[19] Sauer, T. (2012). *Numerical analysis* (2nd ed.). Pearson Education, Inc., p.244-247,316,352,384.

[20] Scheffer M., van Nes E., Holmgren M. and Hughes T. (2008). *Pulse-Driven Loss of Top-Down Control: The Critical-Rate Hypothesis.* Ecosystems, p. 226–237

[21] Stoffers, R. (1984). *The Great Tambora Eruption in 1815 and it's Aftemath.* Science, p.1197

[22] United Nations Population Division (2019). *World Population Prospects 2019 Revision Highlights — United Nations Population Division.* [online] Available at: `https://population.un.org/wpp/Publications/Files/WPP2019_Highlights.pdf`
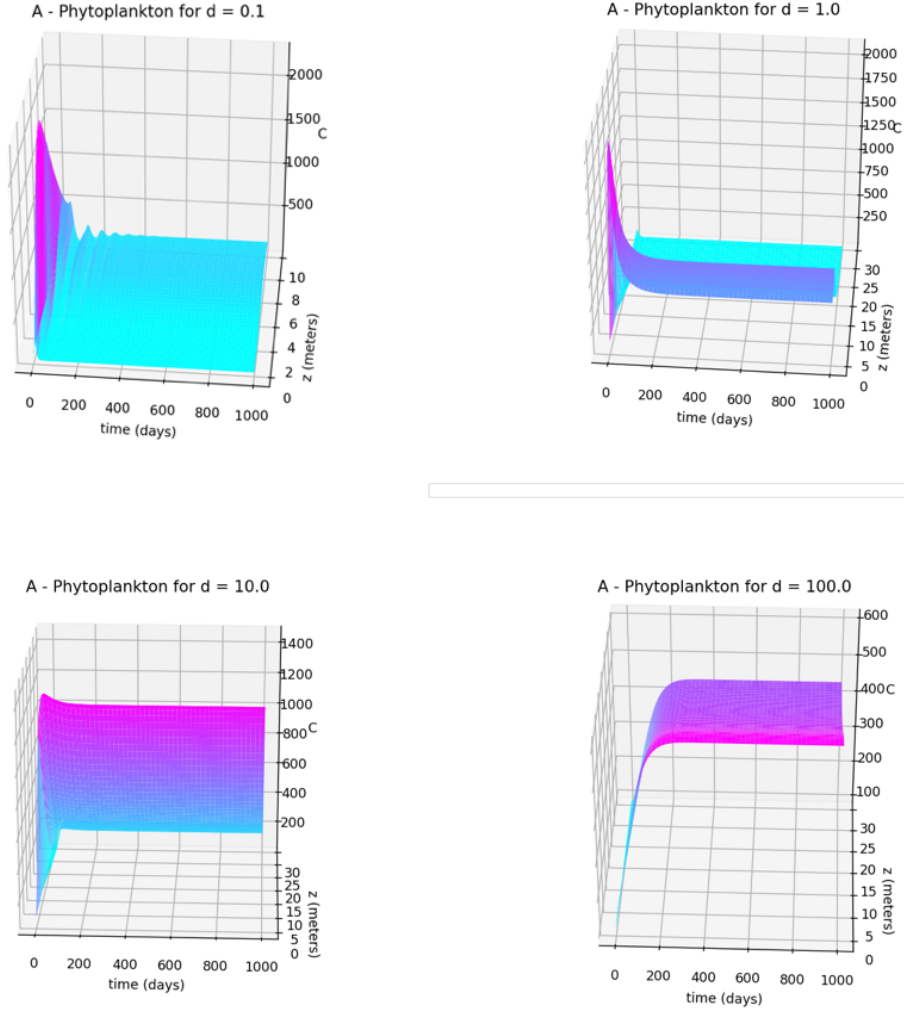
A   Appendix

Figure A1: *Surface plots for different turbulence and water column depth values. Note that the solution generally takes longer to settle into a stationary distribution when there are smaller d-values and larger values of z_{max}, when $z_{max} = 10$ the system settles in under 400 days for $d = 0.1$ as opposed to 800 days when $z_{max} = 30$ in figure 3*
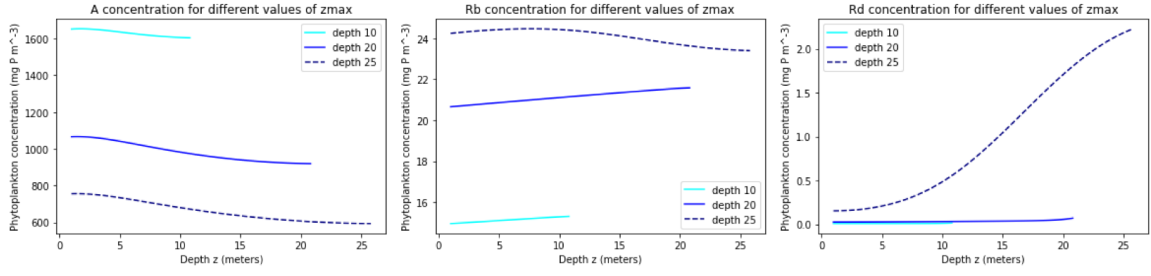
Figure A2: *The distributions of phytoplankton, bound and dissolved nutrients for different water column depths when d=100. Note that A and R_b are always at a maximum or a minimum at z_{max} and R_d is always at a maximum or a minimum at zero. This is in alignment with the Neumann boundary conditions provided in table 2*
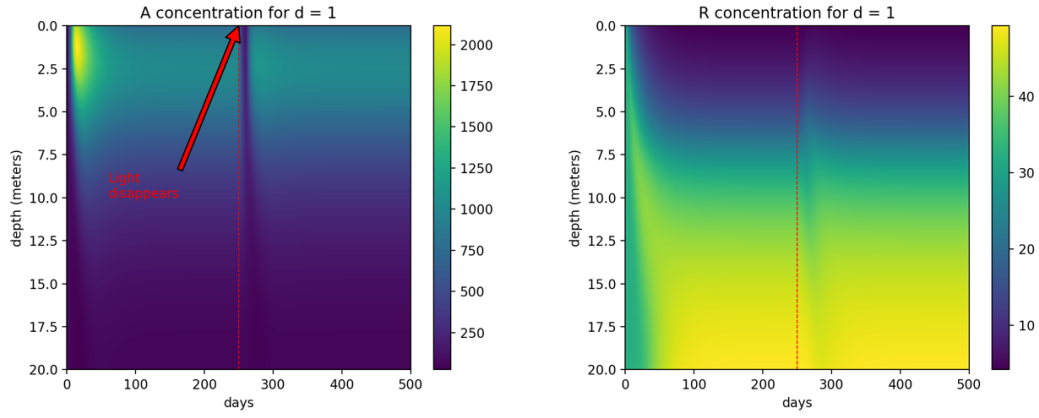

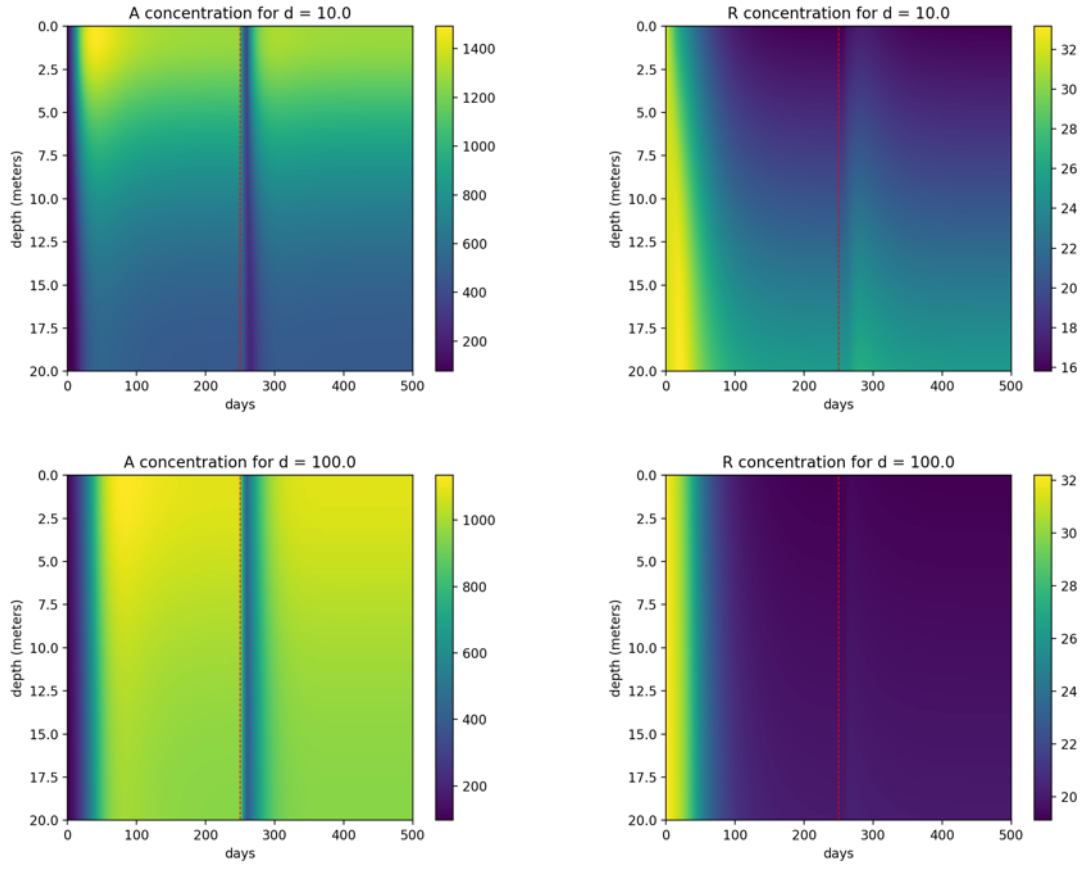Figure A3: *Light disappears for 10 days on the 250th day, d=1, z_{max}=20m*

Figure A4: *Light disappears for 10 days on the 250th day, for d=10 and d=100, z_{max}=20m. For all values of d studied the system has returned to it's stationary distribution within 100 days of the light disappearing for 10 days.*
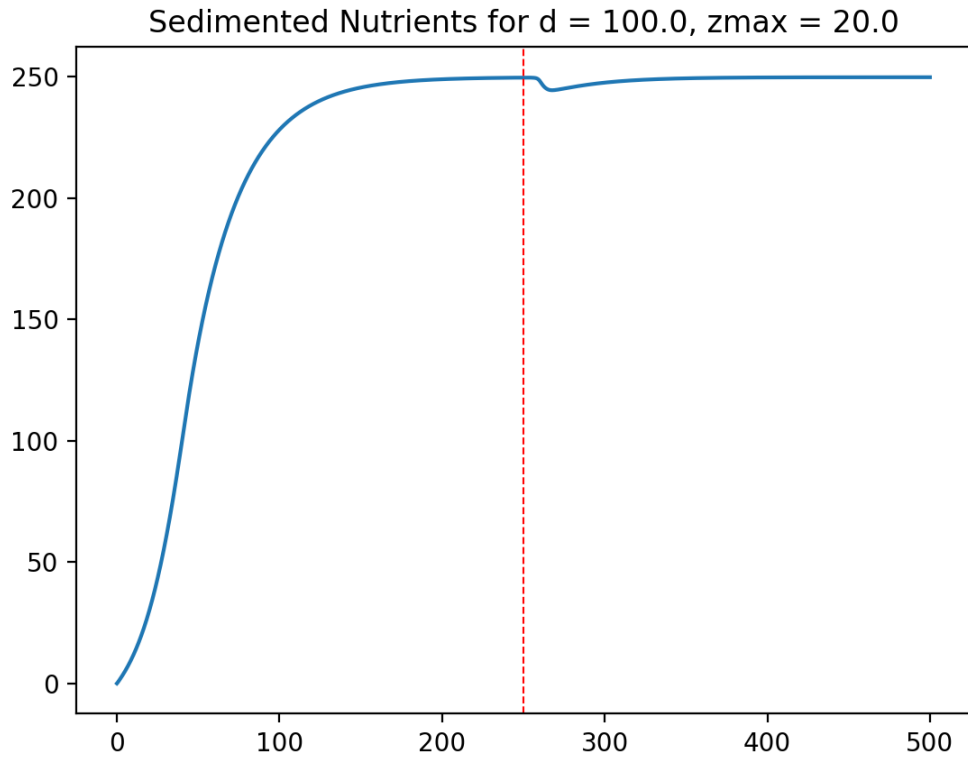
Figure A5: *The value of R_s over time for a water column with depth 20 and turbulence $d = 100$. Light shock occurs for 10 days on day 250. which impacts R_s a few days later as the amount of algae and bound nutrients sinking to z_{max} is insufficient to maintain it's value of around 250 $mg\,P\,m^{-2}$*